

# Naval Research Laboratory

Stennis Space Center, MS 39529-5004



DTIC  
S ELECTE D  
OCT 3 1995  
C

NRL/FR/7240--94-9618

## Semi-Automated Mesoscale Analysis System, Version 1.2: Evaluation Test Results

MATTHEW LYBANON  
SARAH H. PECKINPAUGH

*Remote Sensing Applications Branch  
Remote Sensing Division*

September 28, 1995

19951002 032

Approved for public release; distribution unlimited.

**REPORT DOCUMENTATION PAGE**Form Approved  
OBM No. 0704-0188

Public reporting burden for this collection of information is estimated to average 1 hour per response, including the time for reviewing instructions, searching existing data sources, gathering and maintaining the data needed, and completing and reviewing the collection of information. Send comments regarding this burden or any other aspect of this collection of information, including suggestions for reducing this burden, to Washington Headquarters Services, Directorate for Information Operations and Reports, 1215 Jefferson Davis Highway, Suite 1204, Arlington, VA 22202-4302, and to the Office of Management and Budget, Paperwork Reduction Project (0704-0188), Washington, DC 20503.

<b>1. AGENCY USE ONLY (Leave blank)</b>		<b>2. REPORT DATE</b> September 28, 1995	<b>3. REPORT TYPE AND DATES COVERED</b> Final	
<b>4. TITLE AND SUBTITLE</b> Semi-Automated Mesoscale Analysis System, Version 1.2: Evaluation Test Results			<b>5. FUNDING NUMBERS</b> Job Order No. 572519705 Program Element No. 0603207N Project No. X1596 Task No. Accession No. DN394464	
<b>6. AUTHOR(S)</b> Matthew Lybanon and Sarah H. Peckinpaugh			<b>8. PERFORMING ORGANIZATION REPORT NUMBER</b> NRL/FR/7240--94-9618	
<b>7. PERFORMING ORGANIZATION NAME(S) AND ADDRESS(ES)</b> Naval Research Laboratory Remote Sensing Division Stennis Space Center, MS 39529-5004			<b>10. SPONSORING/MONITORING AGENCY REPORT NUMBER</b>	
<b>9. SPONSORING/MONITORING AGENCY NAME(S) AND ADDRESS(ES)</b> Space and Naval Warfare Systems Command SPAWAR 005 Washington, D.C. 20363-5100				
<b>11. SUPPLEMENTARY NOTES</b>				
<b>12a. DISTRIBUTION/AVAILABILITY STATEMENT</b> Approved for public release; distribution unlimited.			<b>12b. DISTRIBUTION CODE</b>	
<b>13. ABSTRACT (Maximum 200 words)</b> <p>The Naval Research Laboratory's Remote Sensing Applications Branch has developed the Semi-Automated Mesoscale Analysis System (SAMAS), a prototype image analysis system for satellite images of the Gulf Stream region. Previous tests demonstrated that SAMAS shows rudimentary skill in automatically locating the Gulf Stream and its associated eddies. Since those tests, SAMAS has been updated in several ways. This report describes the performance of SAMAS Version 1.2, a newer version that incorporates some new techniques, as well as improvements to some old ones.</p> <p>SAMAS 1.2 was tested by applying it to a set of 22 warmest-pixel composite multichannel sea surface temperature (MCSST) images covering February through June 1993, which were also analyzed by a human expert. The human analyses were regarded as "truth" for the purposes of the statistical analysis of the test results. The human analyses are subjective combinations of analyses from the Naval Oceanographic Office's Warfighting Support Center and information from inspection of the composite images. The analyses, both human and automated, include North Wall positions and eddy definitions, center position coordinates, and sizes.</p> <p>The statistical analysis consists of tabulations and accuracy measures. For eddies, the tabulations compare the number of eddies found by SAMAS versus the number found by the analyst, and the locations and sizes of the eddies. Accuracy measures include position errors and size fractional errors, their first- and second-order statistics (means and standard deviations), as well as minimum and maximum values. The Gulf Stream statistical results were obtained using the same software that was used to evaluate the Gulfcast and Data Assimilation Research and Transition (DART) numerical models. Statistics include information on the longitude range spanned by each Gulf Stream determination, mean position errors, and first- and second-order statistics of the latter.</p>				
<b>14. SUBJECT TERMS</b> satellite remote sensing, expert system, artificial intelligence, automated analysis			<b>15. NUMBER OF PAGES</b> 19	
			<b>16. PRICE CODE</b>	
<b>17. SECURITY CLASSIFICATION OF REPORT</b> Unclassified	<b>18. SECURITY CLASSIFICATION OF THIS PAGE</b> Unclassified	<b>19. SECURITY CLASSIFICATION OF ABSTRACT</b> Unclassified	<b>20. LIMITATION OF ABSTRACT</b> Same as report	

## CONTENTS

EXECUTIVE SUMMARY .....	E-1
1.0 INTRODUCTION .....	1
2.0 SAMAS AUTOMATED PROCESSING .....	2
3.0 STATISTICAL ANALYSIS .....	7
3.1 SAMAS vs. Human Analysis Eddies .....	7
3.2 Gulf Stream Error Analysis .....	8
4.0 CONCLUSIONS .....	15
5.0 ACKNOWLEDGMENTS .....	16
6.0 REFERENCES .....	16

Accession For	
NTIS GPO&J	<input checked="" type="checkbox"/>
DTIC TAB	<input type="checkbox"/>
Unannounced	<input type="checkbox"/>
Justification	
By	
Distribution/	
Availability Codes	
Dist	Avail. and/or Special
A-1	

## EXECUTIVE SUMMARY

The Naval Research Laboratory's Remote Sensing Applications Branch has developed the Semi-Automated Mesoscale Analysis System (SAMAS), a prototype image analysis system for satellite images of the Gulf Stream region. Previous tests demonstrated that SAMAS shows rudimentary skill in automatically locating the Gulf Stream and its associated eddies. Since those tests, SAMAS has been updated in several ways. This report describes the performance of SAMAS Version 1.2, a newer version that incorporates some new techniques, as well as improvements to some old ones.

SAMAS 1.2 was tested by applying it to a set of 22 warmest-pixel composite multichannel sea surface temperature (MCSST) images covering February through June 1993, which were also analyzed by a human expert. The human analyses were regarded as "truth" for the purposes of the statistical analysis of the test results. The human analyses are subjective combinations of analyses from the Naval Oceanographic Office's Warfighting Support Center and information from inspection of the composite images. The analyses, both human and automated, include North Wall positions and eddy definitions, center position coordinates, and sizes.

The statistical analysis consists of tabulations and accuracy measures. For eddies, the tabulations compare the number of eddies found by SAMAS versus the number found by the analyst, and the locations and sizes of the eddies. Accuracy measures include position errors and size fractional errors, their first- and second-order statistics (means and standard deviations), as well as minimum and maximum values. The Gulf Stream statistical results were obtained using the same software that was used to evaluate the Gulfcast and Data Assimilation Research and Transition (DART) numerical models. Statistics include information on the longitude range spanned by each Gulf Stream determination, mean position errors, and first- and second-order statistics of the latter.

SAMAS 1.2 showed some improvement over the earlier version. It found over 80% of the rings the analyst found, with a mean position error of approximately 22 km and a mean fractional size error of 0.165. Gulf Stream mean position errors were in the range of 40-45 km. Gulf Stream statistics were not available for the earlier version, so a comparison is not possible.

## **SEMI-AUTOMATED MESOSCALE ANALYSIS SYSTEM, VERSION 1.2: EVALUATION TEST RESULTS**

### **1.0 INTRODUCTION**

Infrared (IR) satellite images of the ocean provide surface temperature measurements which can be used either to supplement local measurements at various depths obtained by conventional oceanographic techniques or to provide information about areas of the ocean where data from conventional techniques are sparse. Since satellite IR images often depict mesoscale features clearly, the use of such imagery for various oceanographic applications is expanding rapidly. However, present interpretive techniques are largely manual, require significant effort, and are both subjective in nature and highly dependent upon the interpreter's skill. With the proliferation of oceanographic analyses that use satellite data, combined with decreasing Navy manpower levels, it becomes highly desirable for certain applications to move from labor-intensive manual interpretation toward a capability for automated image interpretation.

Over the past several years the Naval Research Laboratory's (NRL) Remote Sensing Applications Branch has developed a prototype image analysis system that shows rudimentary skill in automatically locating both the Gulf Stream and eddies in IR images of the Gulf Stream region. The system is known as the Semi-Automated Mesoscale Analysis System (SAMAS). Some early results are given by Holyer and Peckinpugh (1990). Since that earlier report, continuing development of old techniques, plus the addition of some new ones, have resulted in significant changes to SAMAS.

This report describes evaluation tests of the latest version of SAMAS, Version 1.2, and provides a statistical analysis of the test results. To clarify some of the details, an outline of the processing approach that SAMAS employs is presented here. It is helpful to think of three levels of analysis. The lowest level consists of operations that focus on individual image pixels, without taking advantage of any contextual information. SAMAS' lowest level performs image segmentation. Segmentation is the step that divides an image into regions, which in some cases are objects in the images. Segmentation, in general, can be edge-based or region-based. The output of the lowest level is, therefore, either a set of edges or a set of regions (the regions are bounded by the edges). SAMAS uses an edge-based segmenter known as the cluster shade edge detector (Holyer and Peckinpugh 1989).

The detected edges are passed to an intermediate level which performs two functions, labeling and feature synthesis. Labeling consists of assigning oceanographic identities to the edge fragments created by the segmenter. Feature synthesis combines edge fragments with identical labels into continuous features, at the same time calculating associated parameters such as position and radius. (These two steps could be accomplished with region fragments, but SAMAS 1.2 uses an edge segmenter.) The labeling and feature synthesis functions are a mixture of conventional image processing and artificial intelligence, i.e., some algorithms are pixel-based and some are object-oriented and use contextual information. SAMAS 1.2 offers a choice of two labelers. One is based on nonlinear probabilistic relaxation (Krishnakumar et al. 1990) and one is based on the topography of the image brightness function considered as a surface (Krishnamurthy et al. 1993). The feature

synthesis module for the Gulf Stream uses an expansion of the North Wall in empirical orthogonal functions (EOF) or principal components (Molinelli and Flanigan 1987). That for warm and cold rings fits circles using the circular Hough transform (Duda and Hart 1972).

The highest level consists of an expert system that describes the kinematics of mesoscale features using rules about the time evolution of eddies (both translational motion and size changes) and a neural network that forecasts the coefficients of the EOF expansion at a later time (Thomason 1989; Chase and Holyer 1993; Lybanon 1994). The expert system has two main functions in SAMAS. First, the forecast feature positions can provide approximate feature locations during periods of cloud cover, when direct observation is not possible. Second, the expert system can "update" feature positions from a previous analysis to provide a better first guess for the relaxation labeler.

## 2.0 SAMAS AUTOMATED PROCESSING

The test images are a set of MCSST warmest-pixel composites that cover the period February through June 1993. Each composite consists of one to four images, spanning a 1- to 5-day period. A cloud mask was computed for each image, and a composite cloud mask was created from the individual cloud masks for each of the test images. The method used to create the cloud mask was developed by Gallegos et al. (1993) (see Fig. 1a for an example MCSST warmest-pixel composite image with cloud mask). We acquired the oceanographic analyses for the north Atlantic Ocean covering the test period from the Warfighting Support Center (WSC) of the Naval Oceanographic Office (NAVOCEANO). The analyses include North Wall positions and eddy definitions, center position coordinates, and sizes. The actual days of the WSC analyses do not correspond exactly with the dates of our image data (see Table 1 for image dates and Fig. 2 for WSC dates). For each of the composite images, a human analyst created a subjective analysis consisting of North Wall positions and eddy definitions, based on the composite image and WSC analyses for the composite image time span. These will be referred to as the human analysis.

The first step of the automated processing is edge creation, using the cluster shade edge detector (Holyer and Peckinpaugh 1989). The window size for computing the gray-level co-occurrence (GLC) matrix used to compute the image of cluster shade values is  $16 \times 16$  pixels, and the delta  $x$  and  $y$  values are zero. For every overlapping  $16 \times 16$ -pixel window of the image, a cluster shade value is computed. Using these values, edges are defined. The zero-crossing test is performed as follows: For every overlapping  $3 \times 3$ -pixel window of the image containing the cluster shade values, an initial zero-crossing test for the cluster shade values is done. If within the window there is a value greater than 200 and another value less than -200, an edge is found. The edge is denoted by a value of one at the location of the window's center in the output binary edge image, to be referred to henceforth as the edge image. Once this initial test is done, multiple passes are made through the cluster shade image to extend these edges (up to 30 passes or when no new edges are found). Next, for every overlapping  $3 \times 3$ -pixel window of the cluster shade image, a test is performed. If the center pixel is not already marked as an edge, and any of the other pixels in the window are edge pixels, then the cluster shade values of the window are tested. If there is a value greater than 100 and another value less than -100, an edge is found and thus marked in the edge image.

The last step in the creation of the edge image is a cleaning step. For every overlapping  $16 \times 16$ -pixel window of the edge image, the following test is performed. If the border of the window has no edge marked, but edge points are contained within the window, then the window is "cleaned," i.e., edge pixels are set to zero (see Fig. 1b for an example edge image).

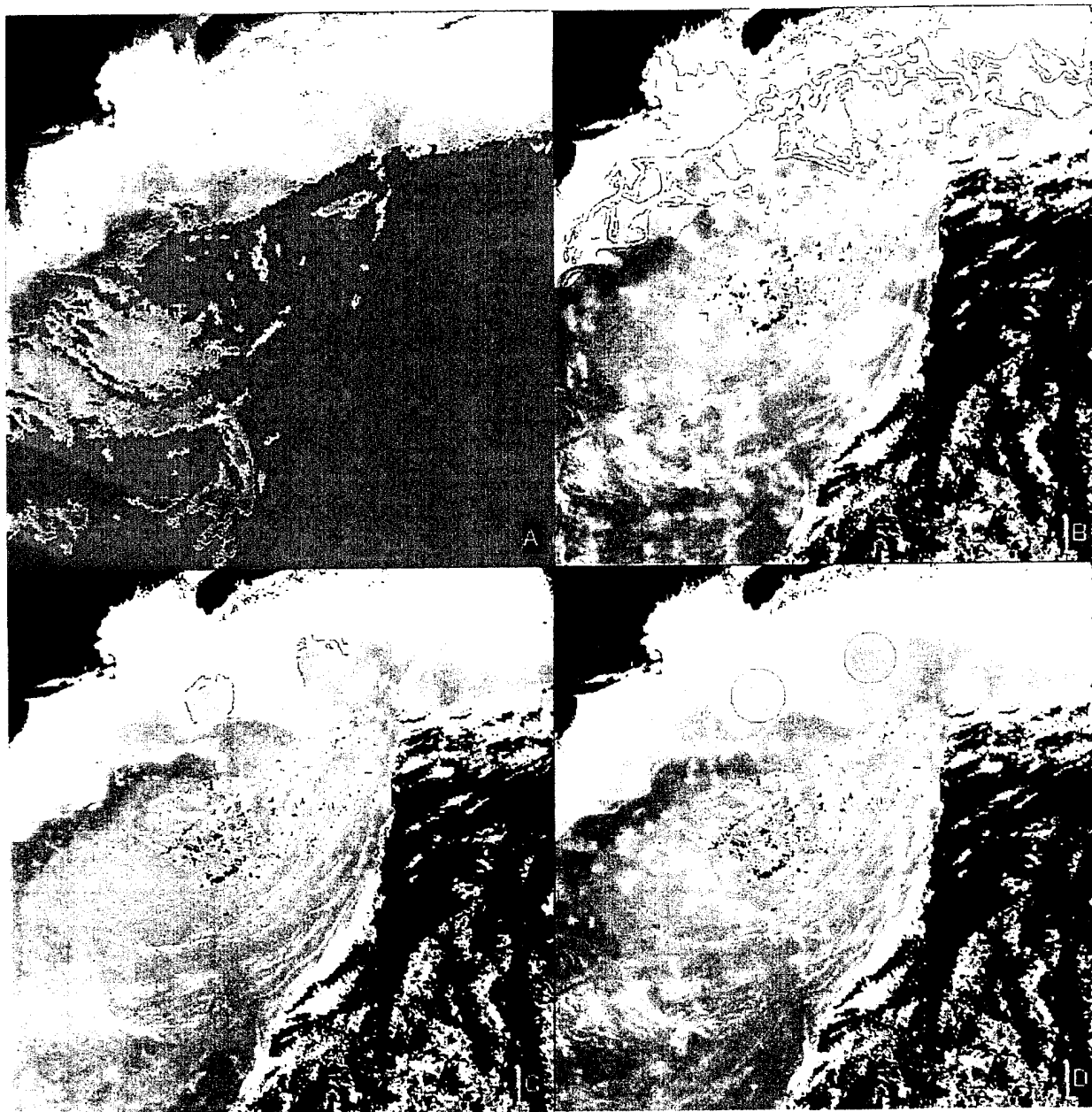


Fig. 1 — (a) MCSST warmest-pixel composite for April 20–24 with composite cloud mask displayed over the image; (b) cluster shade edges displayed over the image; (c) relaxation-labeled edges displayed over the image (yellow for Gulf Stream North Wall edges, red for eddy edges); and (d) CEOF North Wall displayed in yellow, Hough eddies displayed in blue

At this point we have the test image, cloud mask, edges, and human analysis for each of the 22 cases. For edge labeling, the test image, cloud mask, and a previous analysis are needed. With the exception of the first image (in temporal sequence), the previous analysis will be the human analysis from the previous image. For the first image, a WSC analysis will serve as the previous analysis. The next step is to propagate the previous analysis forward in time to match the current image time. The oceanographic expert system accomplishes this task (Lybanon 1990). The expert system depicts expected motions and size changes of warm- and cold-core rings, and their interaction with each other and with the Gulf Stream in the northwest Atlantic Ocean. The

Table 1 — Dates of Images Used for MCSST Warmest Composites.  
Notice that Some Composites Contain Multiple Images from a  
Single Day.

No.	Date Range	Images Used to Create Composite			
1	Mar 1–2	Mar 1	Mar 2	Mar 2	
2	Mar 8–12	Mar 8	Mar 8	Mar 12	
3	Mar 12–16	Mar 12	Mar 16		
4	Mar 21–23	Mar 21	Mar 23		
5	Mar 28–31	Mar 28	Mar 28	Mar 31	
6	Mar 31–Apr 4	Mar 31	Apr 2	Apr 4	
7	Apr 4–7	Apr 4	Apr 6	Apr 7	
8	Apr 7–11	Apr 7	Apr 10	Apr 11	Apr 11
9	Apr 18–20	Apr 18	Apr 19	Apr 20	
10	Apr 20–24	Apr 20	Apr 24		
11	Apr 24–26	Apr 24	Apr 26	Apr 26	Apr 26
12	May 8–10	May 8	May 9	May 9	May 10
13	May 9–12	May 9	May 9	May 10	May 12
14	May 16–19	May 16	May 17	May 18	May 19
15	May 27–28	May 27	May 28		
16	May 28–30	May 28	May 30		
17	Jun 2–5	Jun 2	Jun 5	Jun 5	
18	Jun 9–12	Jun 9	Jun 12		
19	Jun 13–14	Jun 13	Jun 14		
20	Jun 16	Jun 16	Jun 16		
21	Jun 21	Jun 21			
22	Jun 26–27	Jun 26	Jun 27		



February 1993							March 1993						
S	M	Tu	W	Th	F	S	S	M	Tu	W	Th	F	S
1	2	3	4	5	6			<b>1</b>	2	<b>3</b>	4	<b>5</b>	<b>6</b>
7	8	9	10	11	12	13	7	<b>8</b>	9	<b>10</b>	11	<b>12</b>	<b>13</b>
14	15	16	17	18	19	20	14	<b>15</b>	16	<b>17</b>	18	<b>19</b>	<b>20</b>
21	22	23	24	25	26	<b>27</b>	21	<b>22</b>	23	<b>24</b>	25	<b>26</b>	<b>27</b>
28							28	<b>29</b>	30	<b>31</b>			
April 1993							May 1993						
S	M	Tu	W	Th	F	S	S	M	Tu	W	Th	F	S
				1	<b>2</b>	<b>3</b>							<b>1</b>
4	<b>5</b>	6	<b>7</b>	8	<b>9</b>	<b>10</b>	2	<b>3</b>	4	<b>5</b>	6	<b>7</b>	<b>8</b>
11	<b>12</b>	13	<b>14</b>	15	<b>16</b>	<b>17</b>	9	<b>10</b>	11	<b>12</b>	13	<b>14</b>	<b>15</b>
18	<b>19</b>	20	<b>21</b>	22	<b>23</b>	<b>24</b>	16	<b>17</b>	18	<b>19</b>	20	<b>21</b>	<b>22</b>
25	<b>26</b>	27	<b>28</b>	29	<b>30</b>		23	<b>24</b>	25	<b>26</b>	27	<b>28</b>	<b>29</b>
							30	<b>31</b>					
June 1993													
S	M	Tu	W	Th	F	S							
		1	<b>2</b>	3	<b>4</b>	<b>5</b>							
6	<b>7</b>	8	<b>9</b>	10	<b>11</b>	<b>12</b>							
13	<b>14</b>	15	<b>16</b>	17	<b>18</b>	<b>19</b>							
20	<b>21</b>	22	<b>23</b>	24	<b>25</b>	<b>26</b>							
27	<b>28</b>	29	30										

Fig. 2 — Days for WSC analyses (marked bold)

domain is divided into nine regions. The rules that describe the expected behavior of the warm- and cold-core rings differs in each region. For each ring in the analysis, the expert system calculates a new size and center position at a later time. The expert system progresses the Gulf Stream's North Wall in time using a trained neural network rather than rules (Chase and Holyer 1993). Refer to Table 2 for the number of days that the previous analyses are projected in time. Where the number of days is given as zero, the analyses were not processed by the expert system, but used "as is."

The image, corresponding cloud mask and edge image, along with the previous analysis, projected to the image time as needed, are used by the edge-labeling routine to create a new labeled edge image. There are two steps in executing the probabilistic relaxation labeling algorithm (Krishnakumar et al. 1990). In the first step, a priori probabilities are evaluated with the help of a previous, as-needed, time-projected analysis. In the second step, these a priori probabilities are iteratively updated (relaxation) until a consistent labeling is reached. The resulting labeled edge image contains zero values at no edge or discarded edges. One nonzero value is used to represent

Table 2 — Shown for Each Test Image is the Previous Analysis for Labeling Images and Filling in Missing Eddies, Along with the Number of Days Projected by the Expert System for the Analysis. Also Shown is the Previous Analysis for CEOF Modes Creation and Number of Days Projected by the Expert System. All Previous Analyses are Created by the Human Analyst Except Where Specified as WSC.

No.	Image	Previous Analysis Used for Labeling and Eddy Fill-In for Missing Data	No. of Days Projected Forward by Expert System	Previous Analysis Used by CEOF to Create Modes	No. of Days Projected Forward by Expert System
1	Mar 1-2	Feb 27 (WSC)	2	Feb 27 (WSC)	2
2	Mar 8-12	Mar 1-2	6	Mar 1-2	6
3	Mar 12-16	Mar 8-12	0	Mar 1-2	6
4	Mar 21-23	Mar 12-16	5	Mar 12-16	5
5	Mar 28-31	Mar 21-23	5	Mar 21-23	5
6	Mar 31-Apr 4	Mar 28-31	0	Mar 28-31	0
7	Apr 4-7	Mar 31-Apr 4	0	Mar 28-31	0
8	Apr 7-11	Apr 4-7	0	Apr 4-7	0
9	Apr 18-20	Apr 7-11	7	Apr 7-11	7
10	Apr 20-24	Apr 18-20	0	Apr 7-11	7
11	Apr 24-26	Apr 20-24	0	Apr 7-11	7
12	May 8-10	Apr 24-26	12	Apr 24-26	12
13	May 9-12	May 8-10	0	Apr 24-26	12
14	May 16-19	May 9-12	4	May 9-12	4
15	May 27-28	May 16-19	8	May 16-19	8
16	May 28-30	May 27-28	0	May 27-28	0
17	Jun 2-5	May 28-30	2	May 28-30	2
18	Jun 9-12	Jun 2-5	4	Jun 2-5	4
19	Jun 13-14	Jun 9-12	1	Jun 9-12	1
20	Jun 16	Jun 13-14	2	Jun 13-14	2
21	Jun 21	Jun 16	5	Jun 16	5
22	Jun 26-27	Jun 21	5	Jun 21	5

the North Wall of the Gulf Stream, and a different nonzero value is assigned to each eddy (defined by edges) in the output labeled edge image. Figure 1c shows an example of a labeled edge image.

The Gulf Stream North Wall positions are extracted from the labeled image and converted from image-pixel coordinates to latitude and longitude. These positions are then input to the Complex Empirical Orthogonal Function (CEOF) module used for Gulf Stream formation (Molinelli and Flanigan 1987). The CEOF module also uses a Gulf Stream to create a mode file. This Gulf Stream must be of good quality, i.e., the full-length stepwise straight-line interpolation is believable. It is used to "prime" the formation of the current Gulf Stream. Table 2 shows images and the Gulf Stream used to create the required mode file. The number of days used by the expert system to project the human analysis forward in time is the same as that used for the labeling. When a Gulf Stream proves to be unusable for mode file creation, older previous analyses are checked until a suitable Gulf Stream is found (see Fig. 1d for an example of a CEOF-generated Gulf Stream).

The eddy edges are extracted from the labeled edge image to form an eddy edge image. These eddy edges are dilated to double width and then input to the eddy detection routine. The eddy detection uses a modified circular Hough transform (Peckinpaugh and Holyer 1994). Circular features, eddies, are defined by center  $x$ ,  $y$  position and pixel radius sizes. These values are converted to latitude, longitude position and kilometer radius. The Hough transform modification biases the results toward smaller circular features. For each possible radius, an accumulator array image is created (reasonable eddy size for our region is 50–133 km). Each element in the accumulator array image contains the sum of points making up the circle at the corresponding  $x$ ,  $y$  center position of the original image. These values are normalized for the number of points which define a circle of the radius size that corresponds to the accumulator array image. From a series of these accumulator array images, the best (i.e., largest) values are selected. These values define the center position and size values assigned to the eddy. A test is performed to eliminate overlapping of eddies. The test uses a minimum threshold so that 40% of the circle must be defined to detect an eddy. Figure 1d shows an example of Hough transform-defined eddies.

Due to cloud cover in the image, some eddies may not be visible or be defined by clear edges. For this reason, the Hough transform eddies are combined with eddies from the previous analysis. The eddies from the previous analysis, progressed in time by the expert system as needed, are used to fill in eddies not defined by the Hough transform (see Table 2 for previous analysis definitions). A zero value in the "No. of days projected forward by Expert System" column means that no expert system was used for that case. Hough transform eddies are given first priority where there is any overlap with the previous analysis eddies. This combined eddy list defines the eddies for the current image (see Fig. 1d for an example of automated analysis). Note that all eddies for this case were created by the Hough transform.

### 3.0 STATISTICAL ANALYSIS

#### 3.1 SAMAS vs. Human Analysis Eddies

The test data set consisted of 22 images. However, the human expert did not find eddies in nine of the images, so the SAMAS tests employed 13 images for which the analyst found one or more eddies. Let  $E$  = the number of eddies found by the expert in one image, and let  $S = E + N$  = the number of eddies found by SAMAS in one image. Table 3 shows the values of  $N$  for the 13 cases for which the expert found at least one eddy.

Table 3 — Number of Occurrences of Each Value of the Difference  $N$  Between the Number of Eddies Found by SAMAS and the Number Found by the Human Expert

$N$	Number of Images
-7	1
...	...
-5	1
...	...
-2	3
-1	2
0	4
+1	2

Note: For  $N = 0$ , in some cases the SAMAS-found eddies and the analyst-found eddies were not the same eddies (i.e., there were significant differences in their geographical positions).

segment within that longitude range, so that the result is a mean error expressed in kilometers. That program was modified slightly by Dan Fox, and further modified by Matthew Lybanon (both of NRL) to read the SAMAS-format Gulf Stream files. However, the "core" subroutine that performs the error calculation (and other routines called by it) was unchanged, except for one change (by Fox) to compensate for the different sizes of a degree of latitude and a degree of longitude. The original Harvard code failed to compensate for this difference.

The program was set up to perform the calculation over four longitude ranges. That feature was retained and used as described below. The program also requires the data—both ground truth (analyst) and comparison (SAMAS) files—to span the longitude range used in the calculation. Since each file covered a generally different longitude range, in many cases it was necessary to extrapolate the files so that they spanned the largest longitude range used in the analysis. Table 6 illustrates that extrapolation. The left side of the table lists the original longitude limits in each file, and the right side gives the limits after the extrapolation. In every case except one, the method used was linear extrapolation based on the first two or last two points in the file. The exception was for the June 21 "analyst" Gulf Stream, which was very short. It was necessary to extrapolate the western end from  $-59.8077^\circ$  to  $-80.0^\circ$  (a distance greater than the original length). Two points resulting from a linear least-squares fit to the first six points in the original file were necessary to obtain reasonable results.

The most straightforward approach is to compare all the cases over the same longitude ranges. However, it was not clear that this approach was advisable because of the large variations between the longitude ranges actually covered by the different data sets (shown in Table 6). The approach adopted for the analysis is a compromise. The four longitude ranges used in the analysis were split into two pairs of ranges. Two "global" ranges, the same for all data sets, make up the first pair.

There were two cases in which (apparently) the same eddy could be tracked over an extended period, and there were significant discrepancies between the expert and SAMAS values of both position and size. Those two cases are tabulated in Table 4. The abbreviations used in the "Sources" columns in the table are as follows: EE = eddy editor, OC = (NAVOCEANO) Operational Oceanography Center, ED = edge detector, and ES = expert system.

Table 5 gives the position and size errors for each date interval. In the table, "ground truth" values are those found by a human analyst, and "comparison" values are from SAMAS.

### 3.2 Gulf Stream Error Analysis

#### 3.2.1 Means of Evaluation

SAMAS-produced Gulf Stream North Walls are compared with those produced by a human analyst using a program developed by Geraldine Gardner of Harvard University, originally for use in evaluating the Harvard Gulfcast model. The two Gulf Streams are compared over a specified longitude range by interpolating each to a standard grid. The error is estimated by calculating the area between them and dividing that area by the arc length of the ground truth Gulf Stream

Table 4 — Two Cases for Which There were Significant Differences Between SAMAS-Derived and Expert-Derived Eddies

Eddy A							
	Ground Truth			Errors		Sources	
Dates	Lat.	Lon.	Rad.	Pos. (km)	Fract. Size	Expert	SAMAS
24–26 Apr 93	39.1454	–68.419	61.5132	62.25707	–0.01714	EE	ES
16–19 May 93	39.5446	–68.651	39.2824	41.49992	–0.01143	EE	ES
27–28 May 93	39.4251	–69.910	46.9616	66.62056	0.373079	EE	ED
28–30 May 93	39.3852	–69.885	47.2837	20.10504	0.732155	EE	ED
2–5 Jun 93	39.2854	–69.910	45.6201	13.71933	0.743262	EE	ED
13–14 Jun 93	39.3652	–70.347	44.7902	20.70246	0.539013	EE	ED
			Means:	37.48406	0.393157		
Eddy B							
	Ground Truth			Errors		Sources	
Dates	Lat.	Lon.	Rad.	Pos. (km)	Fract. Size	Expert	SAMAS
20–24 Apr 93	40.5100	–65.570	64.8200	15.38535	0.632211	OC	ED
24–26 Apr 93	40.5129	–65.617	73.9719	14.94265	0.231426	EE	ED
8–10 May 93	40.5326	–65.180	37.1211	83.69115	0.764086	EE	ED
9–12 May 93	40.4737	–65.180	37.4276	35.02390	0.632581	EE	ED
16–19 May 93	40.5914	–65.566	66.7426	19.09353	0.015390	EE	ED
27–28 May 93	40.1391	–66.106	60.6521	0	0	EE	EE
28–30 May 93	40.0404	–66.183	71.4185	12.96360	–0.000570	EE	ES
13–14 Jun 93	40.1588	–65.951	51.5543	24.70246	0.539013	EE	ED
16 Jun 93	40.2377	–66.209	48.4476	34.42538	–0.001430	EE	ES
			Means:	26.69200	0.312523		

Notes: (Eddy B) For the 27–28 May 93 data, both the expert and SAMAS values were input by the eddy editor, so they were identical.

(Both eddies) In almost every case, the edge detector found bigger eddies than the expert. This was also true for other eddies in the test cases.

Table 5 — Comparison of SAMAS-Derived Eddies with Those Found by Human Expert

Dates	Ground Truth			Comparison			Position Error (km)	Size Fract. Error
	Lat.	Lon.	Rad.	Lat.	Lon.	Rad.		
Mar 1-2	None							
Mar 8-12	None							
Mar 12-16	None							
Mar 21-23	None							
Mar 28-31	None							
Mar 31-Apr 4	None							
Apr 4-7	None							
Apr 7-11	None							
Apr 18-20	40.552	-65.592	75.275	None				
	41.872	-60.296	82.379	None				
Apr 20-24	None			41.770	-60.300	87.970		
	40.510	-65.570	64.820	40.478	-65.393	105.800	15.385	0.632
	41.770	-60.300	87.970	41.743	-60.228	97.562	6.714	0.109
Apr 24-26	39.145	-68.419	61.513	39.048	-69.129	60.459	62.257	-0.0171
	40.513	-65.617	73.972	40.402	-65.518	91.091	14.943	0.231
	41.949	-60.527	67.980	41.900	-61.150	67.864	51.866	-0.00171
	37.156	-64.666	26.008	41.631	-60.552	89.414	Different Eddies	
May 8-10	40.533	-65.180	37.121	40.593	-66.167	65.485	83.692	0.764
	41.738	-60.682	63.578	41.738	-60.682	63.578	0	0
	38.198	-63.355	22.270	38.198	-63.355	22.270	0	0
	36.578	-64.692	22.986	36.578	-64.692	22.986	0	0
	39.245	-52.661	55.334	39.245	-52.661	55.334	0	0
	None			39.209	-69.985	60.350		

Table 5 — Continued

Dates	Ground Truth			Comparison			Position Error (km)	Size Fract. Error
	Lat.	Lon.	Rad.	Lat.	Lon.	Rad.		
May 9-12	41.661	-60.887	60.114	41.644	-61.094	60.080	17.287	-0.00057
	40.474	-65.180	37.428	40.764	-65.019	61.104	35.024	0.633
	38.259	-63.278	21.210	None				
	36.474	-64.820	24.471	None				
May 16-19	39.545	-68.651	39.282	39.480	-69.127	38.834	41.500	-0.0114
	40.591	-65.566	66.743	40.421	-65.593	67.770	19.094	0.0154
	41.660	-61.299	57.373	41.628	-61.555	55.343	21.592	-0.0354
	33.060	-74.152	35.671	33.040	-74.596	35.589	41.484	-0.00228
May 27-28	38.502	-62.995	31.663	None				
	36.016	-65.232	22.926	None				
	39.425	-69.910	46.962	39.403	-69.136	64.482	66.621	0.373
	35.807	-66.106	32.983	35.807	-66.106	32.983	0	0
May 28-30	40.139	-66.106	60.652	40.139	-66.106	60.652	0	0
	41.235	-62.250	70.113	41.235	-62.250	70.113	0	0
	38.522	-56.260	33.916	38.522	-56.260	33.916	0	0
	39.385	-69.885	47.284	39.209	-69.935	81.903	20.105	0.732
Jun 2-5	40.040	-66.183	71.419	39.989	-66.320	71.378	12.964	-0.00057
	41.196	-62.147	61.469	41.188	-62.250	61.100	8.642	-0.006
	35.786	-66.106	29.727	35.778	-66.201	29.719	8.644	-0.00029
	39.105	-56.312	28.960	None				
Jun 9-12	41.930	-57.828	45.515	40.088	-66.243	60.617	Different Eddies	
	40.650	-64.203	52.428	41.123	-62.524	85.921	Different Eddies	
	40.493	-65.926	50.854	40.115	-66.117	46.802	45.107	-0.0797
	39.285	-69.910	45.620	39.403	-69.960	79.528	13.719	0.743
	38.462	-56.620	42.234	35.799	-66.201	32.973	Different Eddies	
Jun 9-12	41.351	-64.075	50.665	None				
	40.395	-65.720	57.129	None				

Table 5 — Continued

Dates	Ground Truth			Comparison			Position Error (km)	Size Fract. Error
	Lat.	Lon.	Rad.	Lat.	Lon.	Rad.		
Jun 9-12	39.105	-70.399	42.720	None				
	38.401	-57.031	28.713	None				
	41.448	-55.772	36.478	None				
Jun 13-14	39.365	-70.347	44.790	39.248	-70.533	68.933	20.702	0.539
	40.159	-65.951	51.554	40.326	-65.767	80.590	24.273	0.563
	41.467	-63.895	35.152	41.433	-64.010	35.132	10.375	-0.00057
	41.968	-56.800	30.675	41.368	-64.096	56.371	Different Eddies	
	38.603	-56.980	43.578	38.595	-57.079	43.577	8.643	-0.000028
Jun 16	42.026	-56.903	29.546	None				
	41.545	-64.203	47.014	41.424	-63.721	66.753	42.382	0.420
	40.238	-66.209	48.448	40.110	-66.551	48.378	32.425	-0.00143
	38.137	-56.877	41.843	38.117	-57.123	41.840	21.607	-0.000072
Jun 21	None	None						
Jun 26-27	39.644	-66.311	59.217	None				
	41.795	-63.869	47.623	None				
	41.968	-57.057	33.089	None				
	36.764	-67.237	51.917	None				
	39.185	-59.319	65.070	None				
	39.225	-56.517	31.732	None				
	38.360	-52.841	36.192	None				
						Mean	21.972	0.165
						Std. Dev.	21.573	0.278
						Min.	0	-0.0797
						Max.	83.691	0.764

Note 1 — All dates are in 1993.

Note 2 — Eddy center latitude and longitude are in degrees; eddy radius is in kilometers.

Note 3 — A "different eddies" notation means that the "comparison" data set did not contain an eddy corresponding to the one in the "ground truth" data set; the one listed is the comparison eddy closest to the ground truth eddy.



Table 6 — Gulf Stream File Longitude Limits

Date	Original				Extrapolated			
	Analyst		SAMAS		Analyst		SAMAS	
	Min.	Max.	Min.	Max.	Min.	Max.	Min.	Max.
Mar 8-12	-74.8201	-60.6303	-80.0882	-58.5268	-80.0000	-53.0000	Same	-53.0000
Mar 12-16	-74.8458	-67.0825	-80.0636	-58.4649	-80.0000	-53.0000	Same	-53.0000
Mar 21-23	-74.9229	-62.8924	-80.0490	-57.7529	-80.0000	-53.0000	Same	-53.0000
Mar 28-31	-74.8458	-50.5277	-80.1636	-57.9483	-80.0000	Same	Same	-53.0000
Mar 31-Apr 4	-74.9229	-64.4091	-74.6993	-56.5151	-80.0000	-53.0000	-80.0000	-53.0000
Apr 7-11	-74.8972	-50.4763	-75.5156	-58.2901	-80.0000	Same	-80.0000	-53.0000
Apr 18-20	-74.9229	-58.5738	-80.1094	-58.5272	-80.0000	-53.0000	Same	-53.0000
Apr 20-24	-74.7686	-49.6023	-79.8836	-58.3902	-80.0000	Same	-80.0000	-53.0000
Apr 24-26	-74.8972	-54.8721	-80.0190	-58.5644	-80.0000	-53.0000	Same	-53.0000
May 8-10	-74.9229	-57.3142	-79.9709	-58.6314	-80.0000	-53.0000	-80.0000	-53.0000
May 9-12	-74.8715	-57.5198	-80.4305	-59.4863	-80.0000	-53.0000	Same	-53.0000
May 16-19	-74.8972	-56.3887	-80.3070	-58.2478	-80.0000	-53.0000	Same	-53.0000
May 27-28	-74.8201	-53.3297	-80.1542	-60.3940	-80.0000	-53.0000	Same	-53.0000
May 28-30	-74.7686	-53.8952	-74.9946	-57.7872	-80.0000	-53.0000	-80.0000	-53.0000
Jun 2-5	-74.8715	-49.6280	-79.8973	-60.4567	-80.0000	Same	-80.0000	-53.0000
Jun 9-12	-74.8458	-50.1936	-75.7989	-63.6797	-80.0000	Same	-80.0000	-53.0000
Jun 13-14	-74.8201	-50.0650	-80.0183	-59.9915	-80.0000	Same	Same	-53.0000
Jun 16	-74.8715	-51.8130	-80.0056	-59.9575	-80.0000	Same	Same	-53.0000
Jun 21	-59.8077	-49.6280	-79.9960	-58.8618	-80.0000	Same	-80.0000	-53.0000
Jun 26-27	-73.5605	-53.9467	-83.5738	-70.0201	-80.0000	-53.0000	Same	-53.0000

Note 1 — All dates are in 1993.

Note 2 — A "same" entry in an "extrapolated" column means that the value is the same as the one in the corresponding "original" column.

"Global 1," the longer, is  $-79.8^{\circ}$  to  $-54.0^{\circ}$ ; "Global 2" is  $-74.6^{\circ}$  to  $-63.6^{\circ}$ . The values were based on the distributions of endpoint longitudes. Table 7 shows the longitude ranges used as the second pair. They are specific to each data set. The "Special 1" range is always longer than "Special 2."

The Global 1 values were chosen so that, on the average, the SAMAS (generally longer) data ranges prior to extrapolation covered the interval. Global 2 values were chosen so that, again on the average, both SAMAS and analyst data ranges prior to extrapolation covered the interval. Hence, Global 2 is a more conservative choice. Special 1 and Special 2 values were chosen similarly, uniquely for each data set. As a result, Special 2 is a more conservative choice than Special 1.

### 3.2.2 Error Statistics

Table 8 shows the results of the Gulf Stream mean position errors for all four longitude ranges for each data set, as well as the overall means and standard deviations. Global 2 and Special 2 results have comparable mean values, and because of the way the ranges were chosen, the results

Table 7 — Gulf Stream Longitude Ranges  
Specific to Each Date ("Special" Values)

Date	Special 1		Special 2	
	Min.	Max.	Min.	Max.
Mar 8-12	-77.5	-59.6	-72.2	-61.7
Mar 12-16	-77.5	-60.6	-72.2	-70.3
Mar 21-23	-77.5	-60.3	-72.4	-65.5
Mar 28-31	-77.5	-52.4	-72.2	-63.5
Mar 31-Apr 4	-74.8	-60.4	-74.4	-68.4
Apr 7-11	-77.5	-54.5	-72.3	-62.6
Apr 18-20	-77.5	-58.55	-72.3	-58.60
Apr 20-24	-77.3	-51.8	-72.2	-65.0
Apr 24-26	-77.5	-56.7	-72.3	-60.4
May 8-10	-77.5	-58.0	-72.4	-59.3
May 9-12	-77.7	-58.5	-72.1	-60.5
May 16-19	-77.5	-57.3	-72.3	-59.2
May 27-28	-77.5	-56.9	-72.2	-62.2
May 28-30	-74.9	-55.8	-74.0	-59.7
Jun 2-5	-77.7	-55.0	-72.4	-65.9
Jun 9-12	-75.3	-56.9	-74.0	-67.0
Jun 13-14	-77.4	-55.0	-72.2	-65.0
Jun 16	-77.4	-55.9	-72.3	-62.0
Jun 21	-69.9	-54.2	-59.8	-58.9
Jun 26-27	-78.6	-62.0	-73.5	-70.1

Note 1 — All dates are in 1993.

Note 2 — "Global" longitude ranges are  $-79.8$  to  $-54.0$  and  $-74.6$  to  $-63.6$ .

Table 8 — SAMAS Gulf Stream Mean Position Errors

Date	Global 1	Global 2	Special 1	Special 2
Mar 8–12	90.9	44.5	50.2	50.4
Mar 12–16	237.4	99.6	148.5	80.2
Mar 21–23	69.6	59.7	83.7	50.8
Mar 28–31	43.2	59.3	45.7	70.5
Mar 31–Apr 4	103.3	17.9	26.8	22.5
Apr 7–11	56.6	96.9	69.2	92.3
Apr 18–20	44.0	42.2	58.4	59.4
Apr 20–24	50.6	18.8	58.1	19.5
Apr 24–26	56.5	35.9	64.9	67.2
May 8–10	54.9	53.5	61.1	56.4
May 9–12	45.1	16.0	15.0	15.7
May 16–19	30.6	29.5	40.9	41.9
May 27–28	67.0	18.6	49.6	24.2
May 28–30	26.1	13.8	20.1	12.6
Jun 2–5	75.0	26.0	49.7	17.3
Jun 9–12	32.2	22.7	31.2	17.0
Jun 13–14	98.1	12.8	90.1	13.0
Jun 16	69.9	11.9	56.7	17.6
Jun 21	90.6	161.6	112.8	41.3
Jun 26–27	58.4	66.6	57.0	86.4
Mean	70.00	45.39	59.49	42.81
Std. Dev.	45.21	38.03	31.33	26.64

Note 1 – All dates are in 1993.

Note 2 – Column headings for position errors refer to longitude ranges used in calculations.

Note 3 – Position errors are in kilometers.

in those two columns are judged to be more reliable. It is probably best to ignore the other two columns.

#### 4.0 CONCLUSIONS

This study quantifies the feasibility of automated analysis of satellite imagery reported by Holyer and Peckinpaugh (1990) by testing SAMAS on a large data set and providing a statistical analysis of the results. SAMAS 1.2 found over 80% of the rings the human expert found, with a mean position error of approximately 22 km and a mean fractional size error of 0.165. These figures compare favorably with those reported for the earlier version of SAMAS (Holyer and Peckinpaugh 1990). This study also presents quantitative information on the accuracy of Gulf Stream North Wall location for the first time. Gulf Stream mean position errors were in the range of 40–45 km.

## 5.0 ACKNOWLEDGMENTS

Thanks are extended to Bobby Grant of Sverdrup Technology, Inc. for his work processing the data and figure preparation. This work was sponsored by the Space and Naval Warfare Systems Command, CDR D. Markham, Program Manager, under Program Element 0603207N.

## 6.0 REFERENCES

- Chase, J. R. and R. J. Holyer, "Neural Network for Gulf Stream Dynamics," SPIE Vol. 1965, Applications of Artificial Neural Networks IV, 1993, pp. 286-297.
- Duda, R. O. and P. E. Hart, "Use of the Hough Transformation to Detect Lines and Curves in Pictures," *Communications of the ACM* **15**, 11-15 (1972).
- Gallegos, S. C., J. D. Hawkins, and C. F. Cheng, "A New Automated Method of Cloud Masking for Advanced Very High Resolution Radiometer Full-Resolution Data Over the Ocean," *Journal of Geophysical Research* **98**(C5), 8505-8516 (1993).
- Holyer, R. J. and S. H. Peckinpaugh, "Evaluation of the Navy's Semi-Automated Mesoscale Analysis System (SAMAS)," Proceedings of the Fifth Conference on Satellite Meteorology and Oceanography, London, England, September 3-7, 1990 (published by the American Meteorological Society), Boston, MA, 1990.
- Holyer, R. J. and S. H. Peckinpaugh, "Edge Detection Applied to Satellite Imagery of the Oceans," *IEEE Transactions on Geoscience and Remote Sensing* **27**(1), 46-56 (1989).
- Krishnakumar, N., S. S. Iyengar, R. J. Holyer, and M. Lybanon, "Feature Labelling in Infrared Oceanographic Images," *Image and Vision Computing* **8**(2), 142-147 (1990).
- Krishnamurthy, S., S. S. Iyengar, R. J. Holyer, and M. Lybanon, "Topographic Based Feature Labeling for Infrared Oceanographic Images," *Pattern Recognition Letters* **14**(11), 915-925 (1993).
- Lybanon, M. "Tests of an Improved Oceanographic Expert System," NRL/MR/7240--94-7517, Naval Research Laboratory, Stennis Space Center, MS, 1994.
- Lybanon, M. "Oceanographic Expert System Validation Using GOAP Mesoscale Products and Gulfcast/DART Validation Test Data," NOARL Report 5, Naval Research Laboratory, Stennis Space Center, MS, 1990.
- Molinelli, E. J. and M. J. Flanigan, "Optimized CEOF Interpolation of the Gulf Stream," Tech. Report #TR-392395 N66604-86-D-0120 (Subtask 1392-322), Planning Systems, Inc., 1987.
- Peckinpaugh, S. H. and R. J. Holyer, "Circle Detection for Extracting Eddy Size and Position from Satellite Imagery of the Ocean," *IEEE Transactions on Geoscience and Remote Sensing* **32**(2), 267-273 (1994).
- Thomason, M. G., "Knowledge-Based Analysis of Satellite Oceanographic Images," *International Journal of Intelligent Systems* **4**, 143-154 (1989).